Vaccine 33 (2015) 5937–5944

Contents lists available at ScienceDirect

Vaccine

journal homepage: www.elsevier.com/locate/vaccine

Synthetic biology design to display an 18 kDa rotavirus large antigen on a modular virus-like particle

Linda H.L. Lua[a], Yuanyuan Fan[b], Cindy Chang[a], Natalie K. Connors[b], Anton P.J. Middelberg[b,*]

[a] The University of Queensland, Protein Expression Facility, St Lucia, QLD 4072, Australia
[b] The University of Queensland, Centre for Biomolecular Engineering, Australian Institute for Bioengineering and Nanotechnology, St Lucia, QLD 4072, Australia

ARTICLE INFO

Article history:
Available online 19 September 2015

Keywords:
Virus-like particle
Polyomavirus
Computational
Rotavirus
Vaccine

ABSTRACT

Virus-like particles are an established class of commercial vaccine possessing excellent function and proven stability. Exciting developments made possible by modern tools of synthetic biology has stimulated emergence of modular VLPs, whereby parts of one pathogen are by design integrated into a less harmful VLP which has preferential physical and manufacturing character. This strategy allows the immunologically protective parts of a pathogen to be displayed on the most-suitable VLP. However, the field of modular VLP design is immature, and robust design principles are yet to emerge, particularly for larger antigenic structures. Here we use a combination of molecular dynamic simulation and experiment to reveal two key design principles for VLPs. First, the linkers connecting the integrated antigenic module with the VLP-forming protein must be well designed to ensure structural separation and independence. Second, the number of antigenic domains on the VLP surface must be sufficiently below the maximum such that a "steric barrier" to VLP formation cannot exist. This second principle leads to designs whereby co-expression of modular protein with unmodified VLP-forming protein can titrate down the amount of antigen on the surface of the VLP, to the point where assembly can proceed. In this work we elucidate these principles by displaying the 18.1 kDa VP8* domain from rotavirus on the murine polyomavirus VLP, and show functional presentation of the antigenic structure.

1. Introduction

Virus-like particles (VLPs) are an exciting new class of vaccine that have a unique and attractive set of properties including safety, self-adjuvanticity, developability, economy and the ability to be formulated for stability without a cold chain (reviewed in [1]). Their impact on human health is already evident through approved vaccines for Hepatitis B and E and for human papillomavirus. Enormous research interest is now directed towards next-generation modular VLPs, which present parts of a disease-causing pathogen on or within the particle formed from protein of an unrelated virus [2–4]. However, the field of modular VLP design is intellectually immature; design rules for modular VLPs do not yet exist in a way that would enable reliable a priori design of a new vaccine. While critical insights are emerging, for example that immune response quality depends critically on antigen structure [5], it is clear that considerable effort is still required to determine the principles that will lead to reliable rather than serendipitous modular VLP design. Synthetic biology and biomolecular engineering provide tools such as molecular dynamic simulation and process design that will revolutionize the field of VLP vaccine design in coming years [6,7].

Globally, rotavirus continues to impose significant burden of disease, disproportionately on children. Almost half a million of children under five years of age still die from rotavirus infection each year, mostly in developing countries [8]. Two approved live attenuated rotavirus vaccines are available; namely Rotarix™ (GlaxoSmithKline) and RotaTeq™ (Merck). Existing vaccines have significant limitations in the countries of greatest need [9,10]. The affordability of these vaccines in low-income countries and the increased risk of intussusception associated with rotavirus vaccines underpin ongoing research for the next generation of low-cost and safe subunit rotavirus vaccine. The advantages of VLPs mentioned above make them an obvious technology to address this unmet need. VLPs based on the entire virus comprise multiple proteins

* Corresponding author. Tel.: +61 733653609; fax: +61 733469114.
E-mail address: a.middelberg@uq.edu.au (A.P.J. Middelberg).

http://dx.doi.org/10.1016/j.vaccine.2015.09.017

making them difficult to process and characterize [11]. Modular VLPs presenting rotavirus sub-units are a promising approach that brings manufacturing simplicity.

Polyomavirus has proven to be a remarkably efficient and versatile host for presentation of efficacious antigen in a modular fashion [12–15]. We have demonstrated that murine polyomavirus has particular advantage as a modular platform because the protein VP1 can be expressed at high yield in bacterial cells [16] and that this protein can then be assembled, outside of a cell and under process control [17], in a way that is enabling for facile scale-up [18–20]. The result is a process having extremely low manufacturing cost [21] for a VLP that can be formulated to be thermostable [22] presenting modules protective against viral [23,24] and bacterial [25] pathogens.

A limitation in the design of polyomavirus-based VLP vaccines concerns the size of the antigenic module presented. Peptide antigens have been routinely incorporated [3,5,23,26,27] though entire domains have proved more complex. Gleiter et al. [28] have presented a large enzyme on murine polyomavirus, though soluble expression yields were low and enzyme function was reduced presumably due to the incorrect structural conformation of the enzyme. The preferred method for large antigen presentation on polyomavirus has thus evolved to be one based on conjugation to an already-formed VLP, for example through electrostatic interaction [28] or chemical conjugation [29]. This "work-around" of conjugation increases complexity and hence reduces the competitiveness of polyomavirus as a vaccine platform, but is necessary when the principles of large-antigen modular design are not known in a way that allows robust and reliable vaccine design.

In this paper we successfully present the 18.1 kDa VP8* domain [30,31] from rotavirus on the murine polyomavirus VLP platform, by expression of a single modular protein. Using molecular simulation and coupled experiments, we uncover two key design principles that we anticipate will be enabling for the VLP field in general, and for the polyomavirus field specifically. We show that the design of linkers is critical to enable functional separation of the large inserted module from the VLP protein, such that the structures of each are independently maintained. We also show that the incorporation of a large amount of large antigen on the surface of a capsomere, which is the basic building block of a VLP, can inhibit VLP formation, simply because too much antigen is trying to be present on the VLP. This "steric barrier" to VLP assembly was here overcome by co-expressing VP1 protein containing large antigen along with unmodified VP1 protein, i.e., by titrating down the amount of modular antigen on the VLP surface. In this work we used an insect cell expression platform, as this has led to human papillomavirus VLP vaccine approved for human use [32], and because we wished to uncouple the questions of VLP design from those of VLP assembly in vitro. Our subsequent work will extrapolate the principles learned here to the bacterial expression paradigm.

2. Materials and methods

2.1. Homology modelling of capsomeres

Homology models were created using Accelrys Discovery Studio® 3.0. A model of each modular VP1-VP8* protein was first constructed using murine polyomavirus PDB template 1SID for VP1, rotavirus DS-1 strain VP8* core PDB template 2AEN, and Hendra virus glycoprotein PDB template 2 × 9M for Q25 and P6 linker structures. A single modular monomer was modelled within an unmodified capsomere (i.e. 1 × VP1-VP8* and 4 × VP1), to maintain authentic VP1 structure and steric boundaries for antigen presentation, as VP1 exists naturally as a capsomere. Model VP1-VP8* was then further homology modelled into the modular capsomere (i.e. 5 × VP1-VP8*), again using PDB 1SID for capsomere template. Homology model of titrated VP1-VP8* was constructed using two VP1-VP8* monomers and three unmodified VP1 monomers, using PDB 1SID as capsomere template.

2.2. Molecular dynamic simulation of modular VP1-VP8* capsomeres

Molecular dynamics (MD) simulations for capsomeres were performed using GROMACS version 4.6 with Gromos96 43a1 force field and the simple point charge (SPC) model for water. Each all-atom molecular system constructed consisted of a single capsomere, solvated in a cubic box (18 nm^3), with solvent molecules added randomly around polypeptide. The system was solvated using the SPC water model and was neutralized by adding Na^+ counter ions. Berendson method was used to control temperature at 298 K with time constant of 0.1 ps and pressure at 1 atm with coupling constant of 1.0 ps. MD algorithm was used with an integration time step of 2 fs. Particle-mesh Ewald (PME) algorithm was used to account for electrostatic interactions. The cut-offs of neighbour atom list, Coulomb potential, and Lennard–Jones (LJ) potential energies were all set to 1.0 nm. The initial velocities of particles were generated according to a Maxwell distribution at 298.15 K. Then, 5000 steps of steepest descent energy minimization were performed, followed by 100 ps equilibration with position restraints on the protein heavy atoms. The MD simulations were then performed for 20 ns and this simulation process was performed in triplicate for each capsomere. Simulations were performed on Australia's National Computational Infrastructure High Performance Cluster (HPC) Raijin (Fujitsu Primergy HPC), scheduled with a PBS Professional job scheduler, using 128 cores (Intel Xeon Sandy Bridge technology, 2.6 GHz) and 8 GB/core memory for approximately 100 h per simulation.

2.3. Plasmid construction

Transfer vector pBAC™-1 (Merck KGaA, Darmstadt, Germany) carrying modified murine polyomavirus VP1 between *BamHI* and *XhoI* restriction sites was constructed to generate plasmid pBAC-VP1. Murine polyomavirus VP1 sequence (M34958) was modified by site-directed mutagenesis to insert *NaeI* and *AfeI* restriction enzyme sites at positions 86 and 293 of VP1, respectively. The gene fragment encoding human rotavirus outer capsid protein VP8* (2AEN) with flanking GGGGS (G4S) linker sequences was cloned into *AfeI* site of pBAC-VP1, to generate pBAC-VP1-G4S-VP8*-G4S. To construct pBAC-VP1-Q25-VP8*-P6, linker sequences Q25 (residues QGVSDLVGLPNQICLQKTTSTILKP) and P6 (residues PAQCSE) were inserted to flank VP8* gene in plasmid pBAC-VP1-G4S-VP8*-G4S. All constructs were verified by DNA sequencing at the Australian Genome Research Facility (Brisbane, Australia).

2.4. Generation of recombinant baculoviruses

Recombinant baculoviruses were generated using the *flash*BACULTRA™ system (Oxford Expression Technologies, Oxford, UK). *Spodoptera frugiperda* Sf9 insect cells in Sf-900™ II SFM (Life Technologies, California, USA) were seeded at 2.4×10^5 cells/well in a 24-well TC plate. Transfection reaction with a ratio of 20:100 ng *flash*BACULTRA™ baculovirus DNA and each pBAC construct was prepared with Cellfectin® II (Life Technologies, California, USA) and incubated at room temperature for 30 min before dispensing onto the Sf9 cells. The plate was incubated at 27 °C for 5 h before replacing with fresh Sf-900™ II SFM supplemented with 1× antibiotics-antimycotics and incubated at

27 °C for 7 days. Spent medium containing the budded virus was harvested by centrifugation at 1500*g* for 5 min at 4 °C.

2.5. Protein expression

Sf9 cells at mid-log phase of 3×10^6 cells/mL were infected at multiplicity of infection (MOI) of 5 for protein production of VP1 and modular VP1. To investigate the co-infection and co-expression of VP1 and modular VP1-Q25-VP8*-P6, cultures were infected at MOI 1:1, 1:2, 1:3, 1:4 and 1:5 (VP1:VP1-Q25-VP8*-P6). Subsequent co-expression cultures were infected at MOI 1:5 (VP1:VP1-Q25-VP8*-P6). All infected cultures were incubated at 27 °C in a shaking incubator at 120 rpm for 72 h. Cell density and viability were monitored using trypan blue exclusion method and measured on the Countess™ automated cell counter (Life Technologies, California, USA). At harvest, cells were pelleted by centrifugation at 8000 × *g* for 20 min at 4 °C.

2.6. VLP purification

Purification of VLPs using ultracentrifugation was as previously described [33]. For VP1 VLPs, MOPS lysis buffer (50 mM MOPS, 500 mM NaCl, 0.002% (v/v) Tween80, pH 7.0) was used. Tris Base lysis buffer (40 mM Tris Base, 50 mM NaCl, 0.01 mM $CaCl_2$, 0.002% (v/v) Tween 80, pH 8.5) was used for modular VP1 VLPs.

2.7. SDS–PAGE and Western blotting

Protein expression and purification were analyzed using SDS-PAGE gel electrophoresis and Western blotting. Briefly, 4–12% Bis–Tris SDS-PAGE gels (Life Technologies, California, USA) were run according to manufacturer's instructions and visualized by staining with SimplyBlue™ stain (Life Technologies, California, USA). For Western blot analysis, the gel was transferred onto a PVDF membrane and probed with anti-VP1 antibody, followed by goat anti-mouse antibody conjugated with horseradish peroxidase (BD Biosciences, New Jersey, USA). Bands were visualized with enhanced chemiluminescence substrate using a Chemi-Doc™ XRS+ imaging system (Bio-Rad, California, USA).

2.8. Dot blot

Antigens (10 μg) were applied onto a nitrocellulose membrane, blocked with 5% skim milk powder in 0.1% PBST buffer, and probed with either mouse polyclonal antibodies against VP1 or monoclonal antibodies (RV-5:2, [34]) against VP8*. Horseradish peroxidase-conjugated goat anti-mouse antibody was used for detection via chemiluminescence.

2.9. Immunogold labelling

Purified VLP samples (2 μg) were applied onto Formvar-coated grids, left for 2 min, before rinsing with buffer (40 mM Tris Base, 50 mM NaCl, 0.01 mM $CaCl_2$, 0.002% (v/v) Tween 80, pH 8.5) for 1 min to remove excess sample. Grids were blocked with 0.2% fish skin gelatin and 0.2% BSA in buffer for 5 min. Ten times diluted mouse anti-VP8* monoclonal antibody (RV-5:2) was applied and incubated for 30 min at room temperature. After incubation, grids were washed four times with blocking buffer. Gold-conjugated goat anti-mouse antibody was applied and incubated for 30 min at room temperature. After incubation, grids were rinsed with buffer for four times and further washed with water twice. Grids were stained with 2% uranyl acetate for 2 min before visualization under electron microscope.

2.10. Analysis of VLPs

TEM was performed as previously described. Infected cells harvested at 72 h post infection were processed for TEM analysis as described by Lua et al. [35]. For purified VLP samples, 2 μg sample was applied to a Formvar-coated 200-mesh copper grid, stained and visualized as previously described [36]. For VLP size distribution analysis, asymmetric flow field-flow fractionation (AF4) coupled with multi-angle light scattering was performed as described previously [36].

3. Results and discussion

Flexible linkers with residues glycine and serine have been widely used to link peptide or protein in the generation of hybrid proteins [37,38]. Linker G4S was previously used to modularize peptide epitope from group A streptococcus onto VLP [3]. In search of naturally occurring protein domain linkers as seen in [37], linker sequences Q25 (residues QGVSDLVGLPNQICLQKTTSTILKP) and P6 (residues PAQCSE) were derived from the stem region of glycoprotein G (O89343) preceding the beta-propellers globular head and C-terminus region proceeding the globular head, respectively.

Homology modelled VP1-G4S-VP8*-G4S and VP1-Q25-VP8*-P6 capsomere structures were simulated using Gromacs molecular dynamics software for 20 ns. Fig. 1 shows these structures before and after simulation, demonstrating the change in structure at the end of the simulation trajectory. Capsomere VP1-G4S-VP8*-G4S is observed to be collapsing towards the capsomere, with the 18.1 kDa VP8* antigen module folding from above the capsomere down along the side of the capsomere, potentially interacting with VP1 structure, resulting in perturbation of the capsomere structure and showing significant instability. Capsomere VP1-Q25-VP8*-P6 however maintains presentation of the VP8* antigen module above the capsomere with no predicted interaction between antigen and capsomere structure, other than through the purposefully designed linkers. There is no observed capsomere perturbation and the structure of both VP8* antigen and capsomere appear stable. This stability is likely due to the intrinsic flexibility and length of the Q25 and P6 linkers, observed in Fig. 1, providing the antigen and capsomere with enough space to enable maintenance of independent and non-interacting physicochemical characteristics. The short G4S linkers on the VP1-G4S-VP8*-G4S capsomere design provide less flexibility and allow little space between antigen and capsomere potentially activating undesired structural interactions.

Sf9 cultures were infected with recombinant baculoviruses carrying VP1, VP1-G4S-VP8*-G4S or VP1-Q25-VP8*-P6, separately, to determine the expression of each protein. Fig. 2 shows the expression of the unmodified 42.5 kDa VP1 protein as predicted (Lane 2). The theoretical molecular weights of VP1-G4S-VP8*-G4S and VP1-Q25-VP8*-P6 are 61.3 kDa and 64.5 kDa, respectively. A protein band of the correct molecular weight was detected for VP1-Q25-VP8*-P6. However, no VP1-G4S-VP8*-G4S protein was detected by either SDS-PAGE or Western blot analysis (Lane 3). Both cell density and cell morphology post infection suggested that all cultures were well infected, and synchronous infections were achieved since cell growth post infection halted almost immediately [39,40]. These observations confirmed that the linker design has an effect on the expression of modular VP1-VP8* protein.

As reviewed by Chen et al., linkers may improve biological activity, increase expression yield, improve the folding and stability of fusion proteins and target fusion proteins to specific sites in vivo [38]. Molecular dynamic simulation predicts the module VP1-G4S-VP8*-G4S to be unstable and this instability likely affected the expression of the modular protein VP1-G4S-VP8*-G4S, as the extent of expression of a hybrid protein is known to be

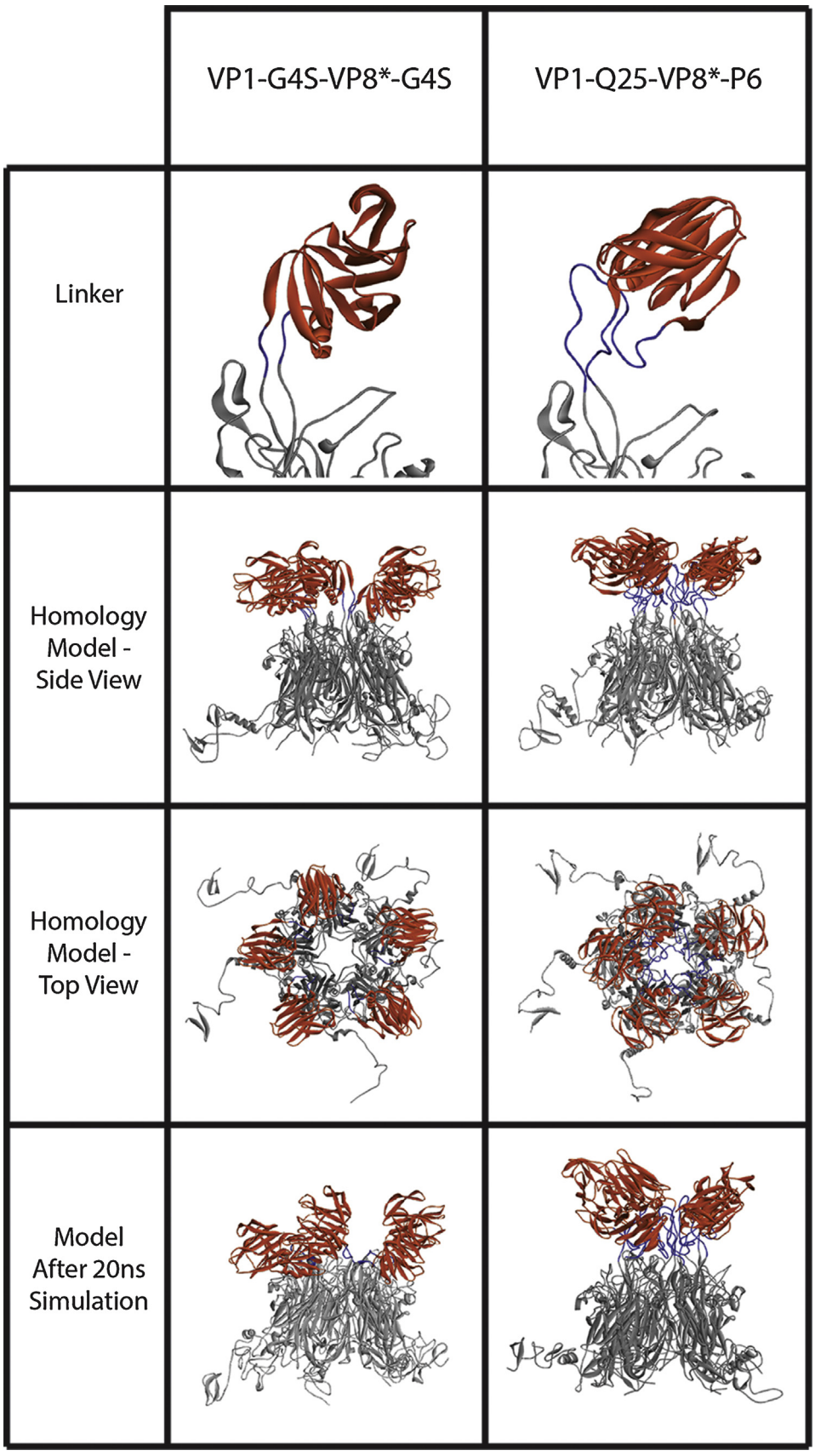

Fig. 1. Effect of linkers on modularizing VP8* on VP1 capsomere. Homology models illustrating the modularization of antigenic module VP8* (red) and flanking linkers (blue) on VP1. (For interpretation of the references to colour in this figure legend, the reader is referred to the web version of this article.)

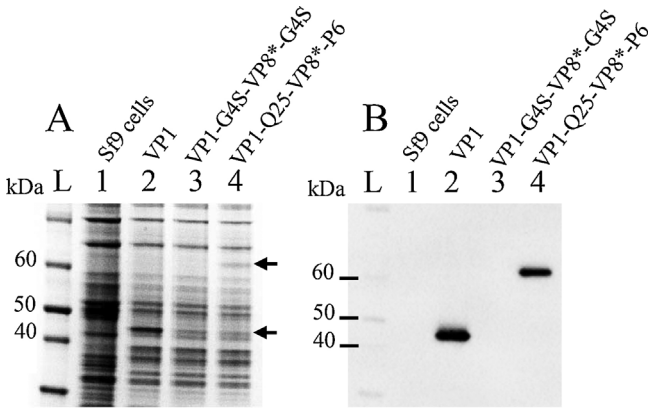

Fig. 2. SDS-PAGE (A) and Western blot (B) analysis on the expression of modular VP1 constructs. Lanes: (L) molecular weight marker; (1) Sf9 non-infected cells; (2) VP1; (3) VP1-G4S-VP8*-G4S; (4) VP1-Q25-VP8*-P6. VP1 proteins migrated at predicted MW 42.5 kDa as indicated by arrow, and VP1-Q25-VP8*-P6 proteins migrated at predicted MW 64.5 kDa (arrow).

sequence- and structure-specific. For example, the effects of linker sequence on expression have been reported for transferrin-based fusion protein, where insertion of linker $(G4S)_3$ did not yield detectable expression but a helical linker $[A(EAAAK)_4A]_2$ gave an 11.2-fold higher production [41].

Ultrathin sections of infected cells were processed and viewed under TEM to examine if assembled VLPs could be observed in the nuclei of cells. As shown in Fig. 3A and B, VP1 VLPs accumulated near the nuclear membrane in the nucleus, similar to previous reports [33]. However, no modular VLP could be seen in cells infected with recombinant baculovirus VP1-Q25-VP8*-P6 although protein expression was confirmed (Fig. 2). It appeared that successful expression of a modular VP1-VP8* protein with permissive linkers did not translate into successful VLP assembly.

We hypothesized that the high density of large antigen modules on the surface of each capsomere (Fig. 1) might have caused a steric barrier, thus preventing VLP assembly. Fig. 4A and B shows the speculative homology model after titrating down the number of antigens present within each assembled capsomere, as would be expected following co-expression of VP1-Q25-VP8*-P6 and VP1. Adverse steric interaction between VP8* antigens is significantly reduced following reduction in the number of VP8* modules per capsomere, potentially enabling a more stable capsomere. More importantly, the combination of flexible purposefully designed linkers and a reduction of modules was predicted to prevent structural perturbation and interference removed by eliminating the steric barrier, allowing the assembly of capsomeres into VLPs.

This hypothesis was tested by adopting the co-expression of VP1 and VP1-Q25-VP8*-P6. A culture of Sf9 cells was co-infected with both recombinant baculoviruses VP1 and VP1-Q25-VP8*-P6 at an MOI ratio 1:5 to compensate for the lower expression of VP1-Q25-VP8*-P6. Both VP1 and VP1-Q25-VP8*-P6 proteins from the co-expressed culture were detected (Fig. 4C, Lane 4). Under TEM, assembled VLPs were observed in the nuclei of co-infected cells

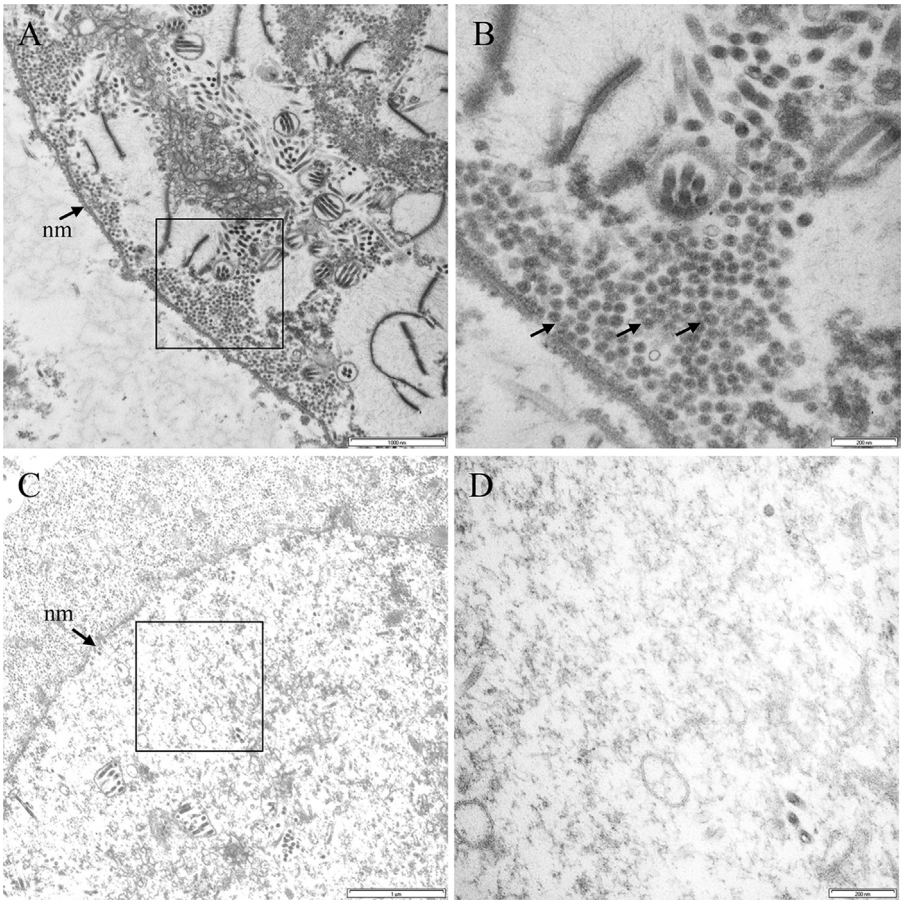

Fig. 3. Electron micrographs of ultrathin sections of infected Sf9 cells. (A) An infected Sf9 cell showing the accumulation of VP1 VLPs in the nucleus, near the nuclear membrane (nm). (B) Arrows indicate assembled VP1 VLPs. (C) Sf9 cell infected with recombinant baculovirus VP1-Q25-VP8*-P6. (D) VLP was not observed in the nucleus of recombinant baculovirus VP1-Q25-VP8*-P6 infected cell.

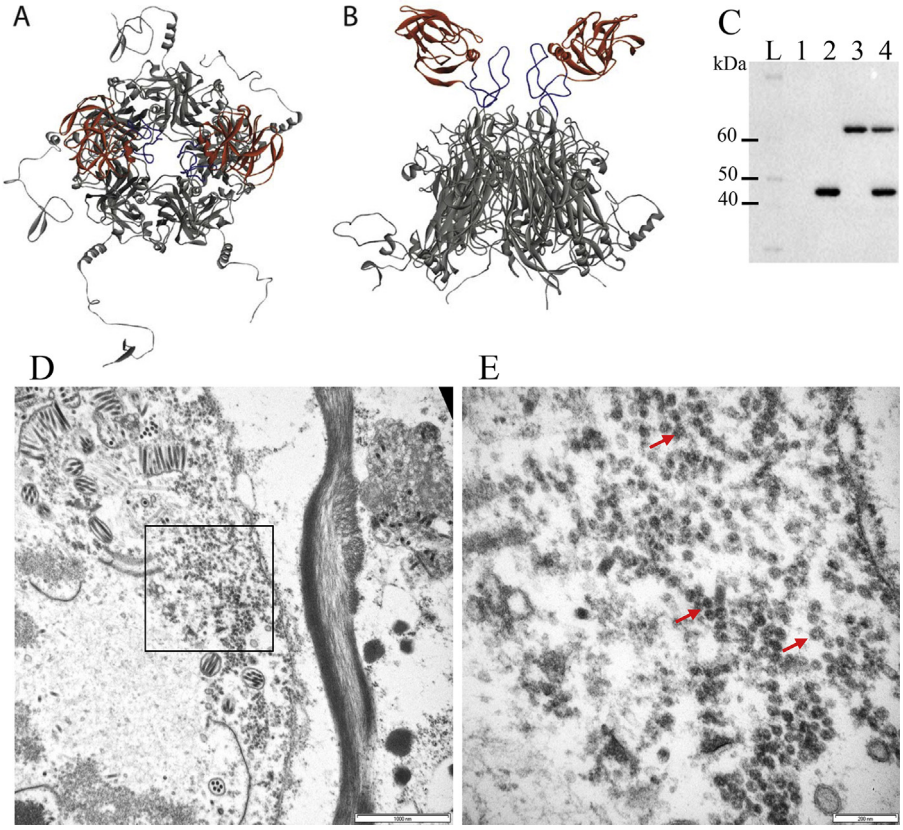

Fig. 4. Co-expression strategy to obtain assembled modular VLPs presenting antigenic module VP8*. (A) Homology model showing the top view of a capsomere (5 VP1 monomers) containing 2 modules of VP8* (red). (B) Side view of a capsomere containing 2 modules of VP8* (red) presented on the surface by linker (blue). (C) Western blot analysis of the expression and co-expression of modular VP1. Lanes: (L) molecular weight marker; (1) Sf9 non-infected cells; (2) VP1; (3) VP1-Q25-VP8*-P6; (4) co-expression of VP1 with VP1-Q25-VP8*-P6. (D and E) Electron micrographs of ultrathin section of Sf9 cells co-infected with recombinant baculoviruses VP1 and VP1-Q25-VP8*-P6. The accumulation of VLPs was observed in the nucleus of infected cell (red arrows). (For interpretation of the references to colour in this figure legend, the reader is referred to the web version of this article.)

and these VLPs were similar in size and morphology to the VP1 VLPs observed in Fig. 3A and B.

Attempts were made to purify VLPs from each expression culture of VP1, VP1-Q26-VP8*-P6 and co-expression VP1:VP1-Q26-VP8*-P6. Fig. 5 shows the banding pattern after caesium chloride density gradient ultracentrifugation. A VLP band was observed in the tube for VP1. In comparison to the VP1 and co-expression VP1:VP1-Q26-VP8*-P6, no VLP band was observed for VP1-Q26-VP8*-P6 in the density gradient tube. This observation further supports the hypothesis that VLP assembly is hindered when a high density of large antigen is present on the surface of a capsomere.

Co-expressed modular VLPs (VLP-VP8*) were purified from the cells using caesium chloride density gradient ultracentrifugation and analyzed under TEM (Fig. 6A). Immunogold labelling with anti-VP8* monoclonal antibodies confirmed that VP8* antigen modules were presented on the surface of these purified VLPs (Fig. 6B). As shown in the dot blot analysis (Fig. 6C), the anti-VP8* antibodies recognise only VP8* module and not the VP1 base. Both immunogold labelling and dot blot analysis with the VP8*-specific rotavirus-neutralizing antibody [34] suggest that modularized VP8* is conformational on the surface of the modular VLPs. Both VP1 VLPs and VLPs-VP8* were of similar size as measured by asymmetric flow-field flow fractionation coupled with multi-angle light scattering (Fig. 6D). The measured radii of unmodified VP1 VLP and VLP-VP8* were 22.4 nm and 22.2 nm, respectively.

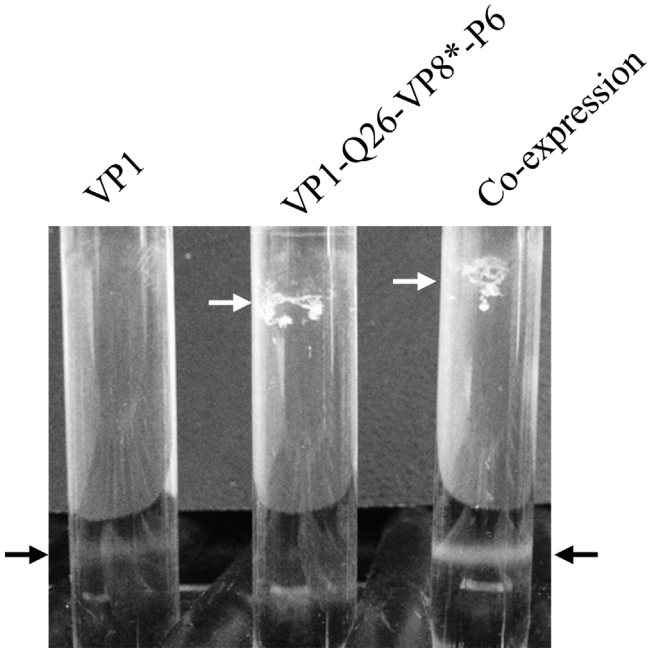

Fig. 5. VLP purification using caesium chloride density gradient ultracentrifugation. Intense bands (black arrows) containing VLPs were observed for VP1 and co-expression samples. No band was detected for VP1-Q25-VP8*-P6. Precipitates (white arrows) were observed in VP1-Q25-VP8*-P6 and co-expression tubes.

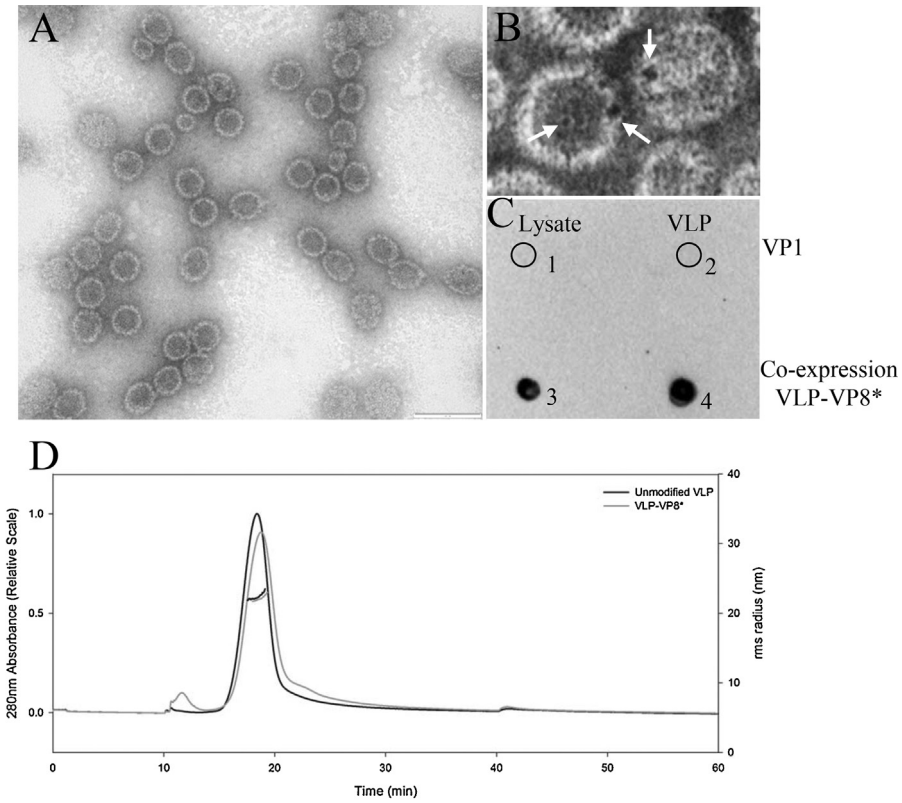

Fig. 6. Analysis of purified modular VLPs presenting VP8* modules, VLP-VP8*. (A) Transmission electron micrograph of ultracentrifuge-purified VLP-VP8* from co-expression. (B) Immunogold labelling with anti-VP8* antibodies detected VP8* modules on the surface of VLPs (arrows). (C) Dot blot analysis with anti-VP8* antibodies: (1) cell lysate of VP1 expression; (2) purified VP1 VLPs; (3) cell lysate of co-expression; (4) purified VLP-VP8*. (D) Asymmetric flow field-flow fractionation fractograms showing the size distribution of VP1 VLPs and VLP-VP8*. (For interpretation of the references to colour in this figure legend, the reader is referred to the web version of this article.)

4. Conclusions

Computational tools were used to investigate the effect of linker on modularizing large antigen on VLP. Results obtained from molecular dynamics simulation were complementary and consistent with the experimental data. The longer flanking linkers, Q25 and P6, provided flexibility for the presentation of the rotavirus VP8* antigen module on VP1, leading to expression of the modular proteins. However, the high density of large antigenic modules on the surface of each capsomere hindered VLP assembly. Assembled modular VLP was obtained using a new module titration strategy by co-expressing unmodified VP1 with modular VP1-Q26-VP8*-P6. This strategy decreased the number of antigenic module per capsomere, thus eliminating the steric barrier. By employing synthetic biology and biomolecular engineering, we have demonstrated the modularization and presentation of 18 kDa rotavirus large antigen on the surface of a manufacturable VLP and, in doing so, revealed two potentially important principles for VLP design.

Acknowledgements

The authors acknowledge research funding under Bill and Melinda Gates Foundation Grand Challenges Explorations (OPP1061405). APJM acknowledges support from the Queensland Government in the form of the 2010 Smart Futures Premier's Fellowship, which also provided salary support for NKC and YF. Computing research was undertaken with the assistance of resources from the National Computational Infrastructure (NCI), which is supported by the Australian Government. APJM thanks Philip Dormitzer and Ethan Settembre for initial discussions on VP8* as a target for VLP presentation. We thank Robert Garcea at the University of Colorado for the plasmid carrying VP1 gene and Barbara Coulson at the University of Melbourne for kind gift of anti-VP8* monoclonal antibody.

Conflicts of interest: The authors declare that there is no affiliation or involvement in an organization or entity with a financial or non-financial interest in the subject matter or materials discussed in this manuscript.

References

[1] Lua LHL, Connors NK, Sainsbury F, Chuan YP, Wibowo N, Middelberg APJ. Bioengineering virus-like particles as vaccines. Biotechnol Bioeng 2014;111:425–40.
[2] Kaczmarczyk SJ, Sitaraman K, Young HA, Hughes SH, Chatterjee DK. Protein delivery using engineered virus-like particles. Proc Natl Acad Sci USA 2011;108:16998–7003.
[3] Middelberg APJ, Rivera-Hernandez T, Wibowo N, Lua LHL, Fan YY, Magor G, et al. A microbial platform for rapid and low-cost virus-like particle and capsomere vaccines. Vaccine 2011;29:7154–62.
[4] Roose K, De Baets S, Schepens B, Saelens X. Hepatitis B core-based virus-like particles to present heterologous epitopes. Expert Rev Vaccines 2013;12:183–98.
[5] Anggraeni MR, Connors NK, Wu Y, Chuan YP, Lua LHL, Middelberg APJ. Sensitivity of immune response quality to influenza helix 190 antigen structure displayed on a modular virus-like particle. Vaccine 2013;31:4428–35.
[6] Pattenden LK, Middelberg APJ, Niebert M, Lipin DI. Towards the preparative and large-scale precision manufacture of virus-like particles. Trends Biotechnol 2005;23:523–9.
[7] Rollié S, Mangold M, Sundmacher K. Designing biological systems: systems engineering meets synthetic biology. Chem Eng Sci 2012;69:1–29.
[8] World Health Organization. Global networks for surveillance of rotavirus gastroenteritis, 2001–2008. Wkly Epidemiol Rec 2008;83:421–8.
[9] Babji S, Kang G. Rotavirus vaccination in developing countries. Curr Opin Virol 2012;2:443–8.
[10] Cherian T, Wang S, Mantel C. Rotavirus vaccines in developing countries: the potential impact, implementation challenges, and remaining questions. Vaccine 2012;30(Suppl. 1):A3–6.

[11] Palomares LA, Ramirez OT. Challenges for the production of virus-like particles in insect cells: the case of rotavirus-like particles. Biochem Eng J 2009;45:158–67.
[12] Gedvilaite A, Frömmel C, Sasnauskas K, Micheel B, Özel M, Behrsing O, et al. Formation of immunogenic virus-like particles by inserting epitopes into surface-exposed regions of hamster polyomavirus major capsid protein. Virology 2000;273:21–35.
[13] Sasnauskas K, Bulavaite A, Hale A, Jin L, Knowles WA, Gedvilaite A, et al. Generation of recombinant virus-like particles of human and non-human polyomaviruses in yeast *Saccharomyces cerevisiae*. Intervirology 2002;45:308–17.
[14] Tegerstedt K, Lindencrona JA, Curcio C, Andreasson K, Tullus C, Forni G, et al. A single vaccination with polyomavirus VP1/VP2Her2 virus-like particles prevents outgrowth of HER-2/neu-expressing tumors. Cancer Res 2005;65:5953–7.
[15] Teunissen EA, de Raad M, Mastrobattista E. Production and biomedical applications of virus-like particles derived from polyomaviruses. J Control Release 2013;172:305–21.
[16] Chuan YP, Lua LHL, Middelberg APJ. High-level expression of soluble viral structural protein in *Escherichia coli*. J Biotechnol 2008;134:64–71.
[17] Chuan YP, Fan YY, Lua LHL, Middelberg APJ. Virus assembly occurs following a pH- or Ca^{2+}-triggered switch in the thermodynamic attraction between structural protein capsomeres. J R Soc Interface 2010;7:409–21.
[18] Liew MWO, Chuan YP, Middelberg APJ. High-yield and scalable cell-free assembly of virus-like particles by dilution. Biochem Eng J 2012;67:88–96.
[19] Liew MWO, Chuan YP, Middelberg APJ. Reactive diafiltration for assembly and formulation of virus-like particles. Biochem Eng J 2012;68:120–8.
[20] Liew MWO, Rajendran A, Middelberg APJ. Microbial production of virus-like particle vaccine protein at gram-per-litre levels. J Biotechnol 2010;150:224–31.
[21] Chuan YP, Wibowo N, Lua LHL, Middelberg APJ. The economics of virus-like particle and capsomere vaccines. Biochem Eng J 2014;90:255–63.
[22] Mohr J, Chuan YP, Wu Y, Lua LHL, Middelberg APJ. Virus-like particle formulation optimization by miniaturized high-throughput screening. Methods 2013;60:248–56.
[23] Wibowo N, Chuan YP, Lua LHL, Middelberg APJ. Modular engineering of a microbially-produced viral capsomere vaccine for influenza. Chem Eng Sci 2013;103:12–20.
[24] Wibowo N, Hughes FK, Fairmaid EJ, Lua LHL, Brown LE, Middelberg APJ. Protective efficacy of a bacterially produced modular capsomere presenting M2e from influenza: extending the potential of broadly cross-protecting epitopes. Vaccine 2014;32:3651–5.
[25] Chuan YP, Wibowo N, Connors NK, Wu Y, Hughes FK, Batzloff MR, et al. Microbially synthesized modular virus-like particles and capsomeres displaying group A streptococcus hypervariable antigenic determinants. Biotechnol Bioeng 2014;111:1062–70.
[26] Chuan YP, Rivera-Hernandez T, Wibowo N, Connors NK, Wu Y, Hughes FK, et al. Effects of pre-existing anti-carrier immunity and antigenic element multiplicity on efficacy of a modular virus-like particle vaccine. Biotechnol Bioeng 2013;110:2343–51.
[27] Rivera-Hernandez T, Hartas J, Wu Y, Chuan YP, Lua LHL, Good M, et al. Self-adjuvanting modular virus-like particles for mucosal vaccination against group A streptococcus (GAS). Vaccine 2013;31:1950–5.
[28] Gleiter S, Stubenrauch K, Lilie H. Changing the surface of a virus shell fusion of an enzyme to polyoma VP1. Protein Sci 1999;8:2562–9.
[29] Kitai Y, Fukuda H, Enomoto T, Asakawa Y, Suzuki T, Inouye S, et al. Cell selective targeting of a simian virus 40 virus-like particle conjugated to epidermal growth factor. J Biotechnol 2011;155:251–6.
[30] Stubenrauch K, Gleiter S, Brinkmann U, Rudolph R, Lilie H. Conjugation of an antibody Fv fragment to a virus coat protein: cell-specific targeting of recombinant polyoma-virus-like particles. Biochem J 2001;356:867–73.
[31] Monnier N, Higo-Moriguchi K, Sun ZYJ, Prasad BVV, Taniguchi K, Dormitzer PR. High-resolution molecular and antigen structure of the VP8* core of a sialic acid-independent human rotavirus strain. J Virol 2006;80:1513–23.
[32] Monie A, Hung C-F, Roden R, Wu TC. Cervarix™: a vaccine for the prevention of HPV 16, 18-associated cervical cancer. Biol: Targets Ther 2008;2:107–13.
[33] Lipin DI, Chuan YP, Lua LHL, Middelberg APJ. Encapsulation of DNA and non-viral protein changes the structure of murine polyomavirus virus-like particles. Arch Virol 2008;153:2027–39.
[34] Fleming FE, Graham KL, Taniguchi K, Takada Y, Coulson BS. Rotavirus-neutralizing antibodies inhibit virus binding to integrins alpha 2 beta 1 and alpha 4 beta 1. Arch Virol 2007;152:1087–101.
[35] Lua LHL, Reid S. Virus morphogenesis of *Helicoverpa armigera* nucleopolyhedrovirus in *Helicoverpa zea* serum-free suspension culture. J Gen Virol 2000;81:2531–43.
[36] Chuan YP, Fan YY, Lua L, Middelberg APJ. Quantitative analysis of virus-like particle size and distribution by field-flow fractionation. Biotechnol Bioeng 2008;99:1425–33.
[37] Argos P. An investigation of oligopeptides linking domains in protein tertiary structures and possible candidates for general gene fusion. J Mol Biol 1990;211:943–58.
[38] Chen XY, Zaro JL, Shen WC. Fusion protein linkers: property, design and functionality. Adv Drug Deliver Rev 2013;65:1357–69.
[39] O'Reilly DR, Miller LK, Luckow VA. Characterizing recombinant gene expression. In: O'Reilly DR, Miller LK, Luckow VA, editors. Baculovirus expression vectors a laboratory manual. New York, NY: Oxford University Press; 1994. p. 180–215.
[40] Wong KTK, Peter CH, Greenfield PF, Reid S, Nielsen LK. Low multiplicity infection of insect cells with a recombinant baculovirus: the cell yield concept. Biotechnol Bioeng 1996;49:659–66.
[41] Amet N, Lee HF, Shen WC. Insertion of the designed helical linker led to increased expression of Tf-based fusion proteins. Pharm Res-Dord 2009;26:523–8.